AD_____

Award Number: W81XWH-10-1-0702

TITLE: Promoting Cartilage Stem Cell Activity to Improve Recovery from Joint Fracture

PRINCIPAL INVESTIGATOR: James A. Martin PhD

CONTRACTING ORGANIZATION: The University of Iowa
Iowa City, IA 52242

REPORT DATE: March 2012

TYPE OF REPORT: Annual

PREPARED FOR: U.S. Army Medical Research and Materiel Command
Fort Detrick, Maryland 21702-5012

REPORT DOCUMENTATION PAGE

Form Approved
OMB No. 0704-0188

1. REPORT DATE *(DD-MM-YYYY)*	2. REPORT TYPE	3. DATES COVERED *(From - To)*
01-03-2012	Annual	27 SEP 2011 - 26 FEB 2012

4. TITLE AND SUBTITLE
Promoting Cartilage Stem Cell Activity to Improve Recovery from Joint Fracture

5a. CONTRACT NUMBER

5b. GRANT NUMBER
W81XWH-10-1-0702

5c. PROGRAM ELEMENT NUMBER

6. AUTHOR(S)

James A. Martin, PhD

Yuki Tochigi, MD, PhD

5d. PROJECT NUMBER

5e. TASK NUMBER

5f. WORK UNIT NUMBER

7. PERFORMING ORGANIZATION NAME(S) AND ADDRESS(ES)

University of Iowa
Iowa City, Iowa 52242-1100

8. PERFORMING ORGANIZATION REPORT NUMBER

9. SPONSORING / MONITORING AGENCY NAME(S) AND ADDRESS(ES)
U.S. Army Medical Research and
Materiel Command, Fort Detrick,
Maryland 21702-5012

10. SPONSOR/MONITOR'S ACRONYM(S)

11. SPONSOR/MONITOR'S REPORT NUMBER(S)

12. DISTRIBUTION / AVAILABILITY STATEMENT

Approved for public release; distribution unlimited

13. SUPPLEMENTARY NOTES

14. ABSTRACT

It has been assumed that chondrocytes killed by mechanical injury to articular cartilage are never replaced and that the resulting hypocellularity contributes to post-traumatic osteoarthritis. However, we found that nonviable areas in an explant injury model were repopulated within 7-14 days by cells that appeared to migrate from the surrounding matrix. We hypothesized that the migrating population included chondrogenic progenitor cells drawn to injured cartilage by alarmins released from dead chondrocytes.

Injuries that caused chondrocyte death stimulated the emergence and homing of chondrogenic progenitors via RAGE-mediated chemotaxis. Moreover, when supplied with a fibrin matrix chondrogenic progenitor cells regenerated cartilage in a chondral defect. Thus, we confirmed an endogenous mechanism that may be leveraged to repair cartilage defects *in vivo* that might otherwise lead to progressive cartilage loss.

15. SUBJECT TERMS
Chondrogenic progenitor cells, chemotaxis, cartilage repair

16. SECURITY CLASSIFICATION OF:			17. LIMITATION OF ABSTRACT	18. NUMBER OF PAGES	19a. NAME OF RESPONSIBLE PERSON
a. REPORT	b. ABSTRACT	c. THIS PAGE			USAMRMC
U	U	U	UU	34	19b. TELEPHONE NUMBER *(include area code)*

Table of Contents

Page

1. INTRODUCTION

This proposal is concerned with enhancing the environment for healing of articular cartilage following joint injury. Recent findings suggest that chondrogenic progenitor cells (CPC) with stem cell-like characteristics may be capable of cartilage repair in the context of mechanical injury. Learning to leverage this potential for endogenous repair could provide a novel, relatively non-invasive intervention to prevent the pathogenesis of PTOA.

2. BODY

Experiments performed in this project yielded a number of significant and surprising results. Many of the findings that flowed from the award are detailed in the accompanying manuscript *Chondrogenic Progenitors Respond to Cartilage Injury* (Appendix 1), which was recently re-submitted to Arthritis and Rheumatism after a first round of largely favorable reviews. Pertinent data that were not included in the manuscript are presented in this report.

2.1 Characterization of CPCs in injured cartilage

Initially we observed migrating cells emerging on top of cartilage that had been injured by blunt impact **(Figure 1)**. As outlined in Aims 2 and 3, we focused on characterizing these injury-responsive migrating cells. These analyses showed unequivocally that the migrating cells were chondrogenic progenitor cells (CPCs) as defined in the literature **(Figure 2)**.

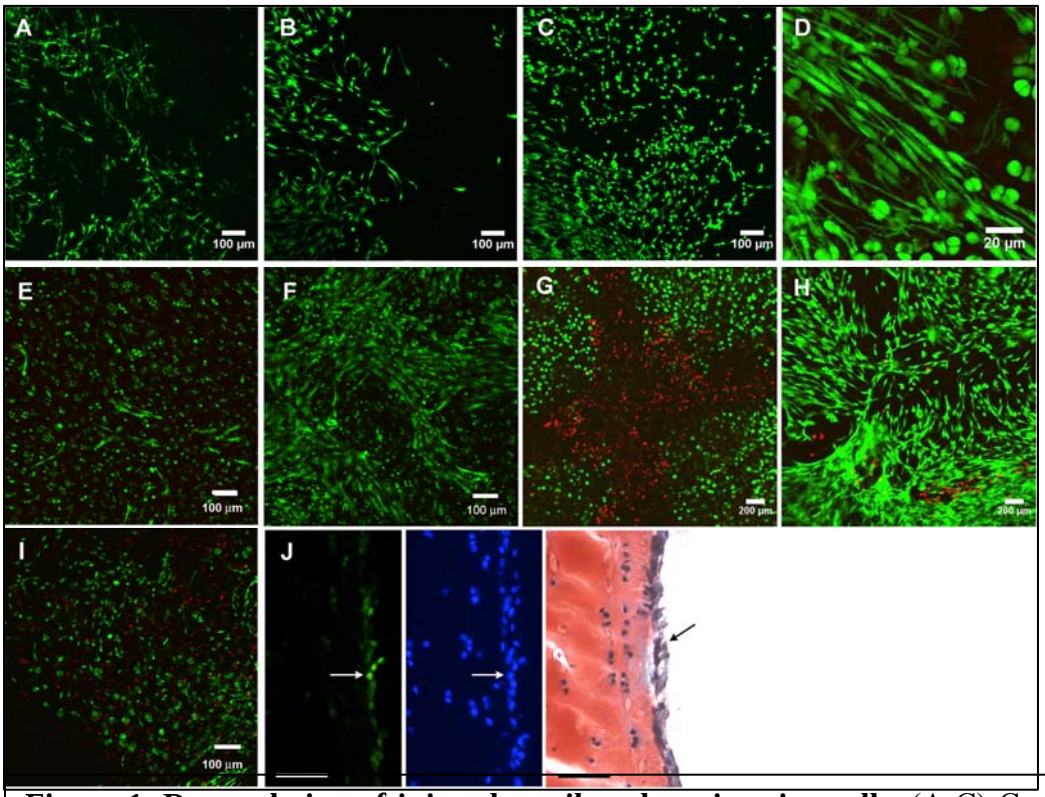

Figure 1. Repopulation of injured cartilage by migrating cells. (A-C) Confocal images show the same area within an impact site on the surface of a bovine tibial plateau explant stained with calcein AM at 7 days (A), 11 days (B), and 15 days (C) post-impact. The elongated morphology and dendritic appearance of the migrating cells are shown in a high magnification view (D). Confocal images of an impact site on a human talus from a 36 year old male at 6 days (E) and 10 days (F) post-impact. The images in G and H show dead chondrocytes (red) and live chondrocytes (green) in a bovine explant with a cross-shaped needle scratch. The explant was stained and imaged immediately after the injury (G) and 14 days after injury (H). Migrating cells were observed on the surfaces of cartilage dissected free from subchondral bone immediately after impact (I). (J) Green immunofluorescence staining for PCNA reveals positive cells (arrow) on the surface of a cartilage explant (left panel). The blue staining (middle panel) shows all nuclei in the same section. Surface-migrating pCPCs (arrow) can be seen in a consecutive section stained with safranin-O (right panel). The bars at the bottom of the left and right panels indicate 100 microns.

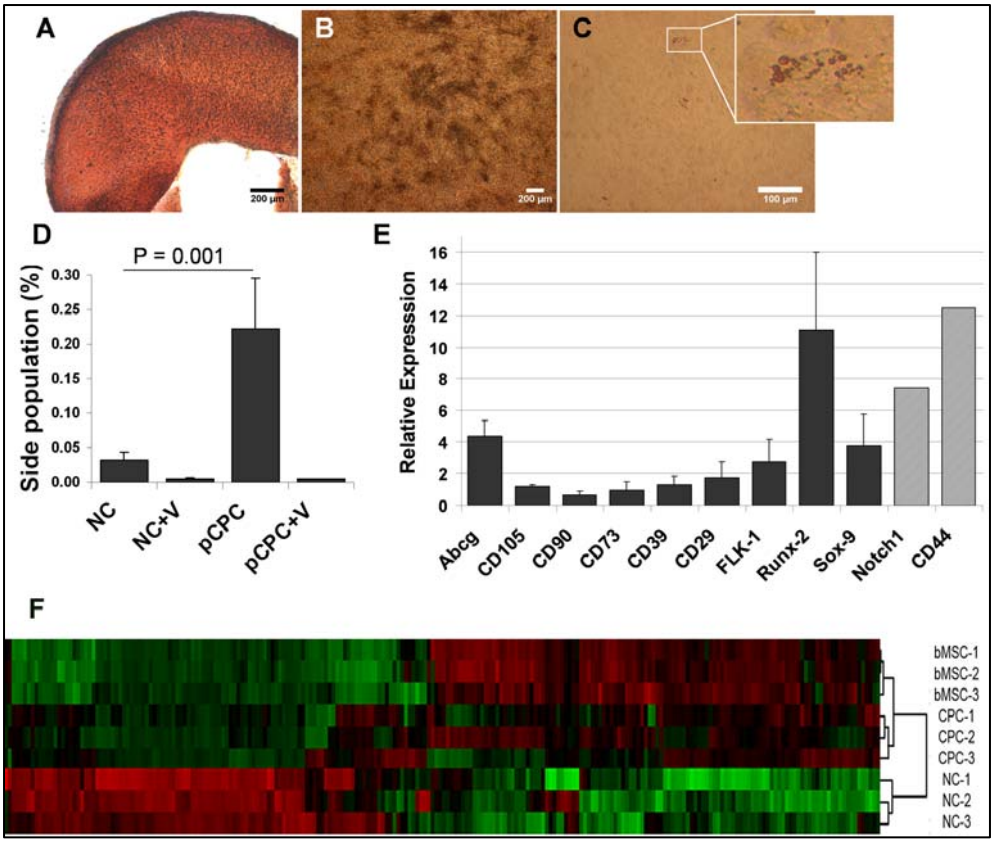

Figure 2. pCPCs show stem cell characteristics. (A-C) pCPCs were cultured under chondrogenic (A), osteogenic (B), and adipogenic (C) conditions. The pellet culture showed intense red Safranin-O/fast green staining indicating the presence of cartilage proteoglycans. (B) Deposition of calcium phosphate was detected by staining with Alizarin Red (dark red spots). (C) Only a few cells produced positive fat vacuoles in Oil Red O staining. (D) FACS analysis showed that the proportion of SP was significantly higher in progenitor cells than in chondrocytes (p=0.001). As expected Verapamil (V), an ABCG transport inhibitor, ablated the side population. (E) The graph shows real-time PCR analysis (dark columns) and microarray analysis (light columns) of marker gene expression in pCPCs relative to NCs (fold change). (F) A heatmap and dendrogram summarize microarray data for the indicated cell populations (triplicate analyses). Colored bars show genes that were expressed at higher or lower levels than the median value (green and red respectively). The dendrogram on the right indicates that CPCs and BMSCs were more closely related to each other than to NCs.

We found evidence to suggest that these cells originated in superficial zone of cartilage, but a firm conclusion awaits more definitive experiments that are currently underway (Section 2.5). Global analysis of gene expression revealed that the CPCs were more closely related to mesenchymal stem cells (MSCs) than to normal chondrocytes **(Figure 2F, Table)**. However, CPCs expressed cartilage matrix genes at higher levels than MSCs, particularly with regard to PRG4/lubricin, a critical surface lubricant made by superficial chondrocytes. This suggested that CPCs may be involved in replenishing lubricants lost as a result of injury, an activity that could help to compensate for the proteolytic loss of PRG4 and the decimation of superficial chondrocytes induced by mechanical injury. In pellet cultures under chondrogenic conditions, CPCs readily formed a cartilage-like matrix. In an explant model CPCs from the surrounding cartilage invaded fibrin-filled chondral defects and produced proteoglycans, suggesting they may be capable cartilage regeneration **(Figure 3)**. Dr Seol, who was awarded a Ph.D. for his work related to this project, is pursuing optimization studies to determine if the cells can be coaxed to accelerate matrix production. These studies have focused on improving CPC infiltration in defects by brief collagenase digestion of cartilage surrounding defects and using hydrostatic or axial loading to promote chondrogenic activity.

Gene Symbol	CPC v NC Δ	p value	Gene Symbol	CPC v MSC Δ	p value
IL6	**130**	*3.6E-05*	PRG4	**78**	*7.6E-05*
DOCK10	**62**	*4.4E-07*	MMP3	**23**	*1.0E-03*
CXCL8	**36**	*3.0E-03*	ACAN	**17**	*5.4E-04*
CCNB1	**35**	*5.8E-05*	S100A1	**16**	*2.7E-04*
CXCL12	**28**	*2.4E-05*	MMP1	**15**	*5.2E-03*
CSF1	**21**	*9.3E-06*	HAPLN1	**13**	*1.0E-05*
MMP1	**18**	*3.9E-03*	S100A1	**13**	*1.7E-04*
CD44	**12**	*6.1E-03*	CXCL2	**12**	*2.0E-02*
ADAMTS4	**10**	*2.9E-05*	IL8	**10**	*2.5E-02*
IL1RN	**9**	*1.3E-04*	COL2A1	**6.9**	*8.0E-05*
CCND1	**9**	*2.3E-05*	SOD3	**6.7**	*1.3E-04*
ADAM9	**6**	*1.6E-03*	COL5A3	**6.2**	*1.5E-03*
IGFBP3	**6**	*2.7E-02*	FGF2	**5.1**	*8.6E-05*
MMP13	**4**	*1.2E-02*	IL16	**3.3**	*8.5E-03*
HMMR	**4**	*1.4E-04*	CD83	**3.2**	*1.5E-02*
TLR3	**4**	*3.7E-02*	PLAT	**3.0**	*4.2E-02*
ITGB5	**4**	*4.0E-02*	IL1A	**2.7**	*2.2E-02*
COL6A1	**3**	*1.1E-02*	S100B	**2.6**	*1.6E-03*
ADAM8	**3**	*2.0E-02*	PDGFRA	**2.5**	*8.4E-03*
COL10A1	**-192**	*7.0E-06*	NID1	**-11.4**	*4.4E-02*
CHAD	**-136**	*1.5E-08*	IGFBP7	**-10.1**	*6.7E-03*
COL9A2	**-38**	*4.9E-06*	PPARG	**-9.8**	*5.3E-03*
COL2A1	**-12**	*9.8E-06*	THBS1	**-6.5**	*4.2E-02*
TIMP4	**-8**	*9.4E-05*	GPC4	**-6.2**	*1.8E-02*
ACAN	**-8**	*5.2E-03*	IGFBP3	**-5.4**	*4.6E-02*
INSR	**-6**	*1.7E-03*	IGFBP2	**-3.6**	*1.0E-02*
COMP	**-5**	*4.9E-04*	IL1RN	**-3.6**	*4.3E-03*
TIMP4	**-5**	*9.7E-04*	PLAU	**-3.0**	*2.0E-03*
COL2A1	**-4**	*2.5E-03*	DNMT3A	**-2.7**	*1.1E-02*
FGF2	**-4**	*3.2E-04*	IGFBP4	**-2.6**	*2.6E-02*
ACAN	**-4**	*3.2E-02*	NOTCH1	**-2.3**	*6.2E-04*
PTH1R	**-3**	*1.8E-02*	ADAM10	**-2.0**	*6.6E-02*

Table. Relative Gene Expression. Positive and negative fold change (Δ) for pCPC versus NC (left) and CPC versus BMSCs (right) are shown together with p values (italics). The list includes genes expressed at levels that were at least 2-fold higher (top) or lower (bottom) in pCPCs.

2.2 Mechanisms of CPC chemotaxis

One way to boost the regenerative capacity of CPCs is to enhance their recruitment to injured cartilage. Although initial studies indicated that the cells were migrating toward fractured cartilage, it was unclear what they were responding to. Thus, we delved into the mechanisms of CPC chemotaxis. In the beginning we noticed that almost any insult that resulted in substantial chondrocyte death provoked CPC emergence. A series of chemotaxis assays revealed that CPCs were highly reactive to factors present in chondrocyte lysates. Further analysis showed that the nuclear protein high-mobility group box 1 (HMGB1), one of several chemotactic "alarmins" released by dead cells, was a key factor **(Figure 3)**. The response to HMGB1 in CPCs was mediated by the receptor for advanced glycation end products (RAGE), an innate immune system receptor. These data suggest that HMGB1 could be used to attract increased numbers of CPCs to cartilage injuries.

2.3 Potential to exacerbate joint inflammation

The data described above seemed to support a potential reparative role for CPCs in damaged cartilage. However, additional analyses of CPC gene expression and cell behavior led us to consider a pathogenic role for CPCs. CPCs over-expressed genes encoding collagenases and other matrix proteases associated with osteoarthritis (OA). Moreover, they vastly over-expressed interleukin-6 (IL-6), and chemokines known to promote leukocyte infiltration (CXCL8, and CXCL12) **(Table)**. Thus there is a potential for CPCs to act as initiators and amplifiers of inflammation in injured joints. These observations filled a knowledge gap that allowed us to put forward a plausible mechanism for how intra-articular cell death contributes to post-traumatic synovitis: 1. Cells killed by joint injury release alarmins that activate CPCs locally. 2. CPCs amplify this signal through rapid proliferation and mass production of chemokines. 3. Chemokine levels in synovial fluid rise to levels that cause leukocyte infiltration resulting in synovitis.

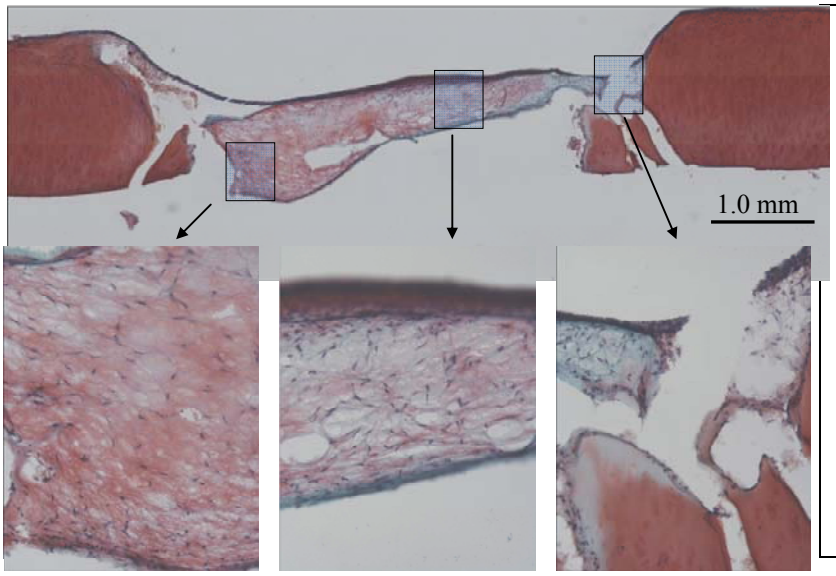

Figure 3. Invasion and matrix formation by CPCs in a fibrin-filled cartilage defect. A safranin-O stained cryosection was cut through a 5 mm fibrin-filled chondral defect after 2 weeks of incubation. The defect is flanked by dark-staining native cartilage. White arrows point to a continuous sheet formed by CPCs on the defect surface and surrounding cartilage. The inset panels show that the originally cell-free fibrin filler i populated by CPCs that invaded the matrix and began to secrete proteoglycans.

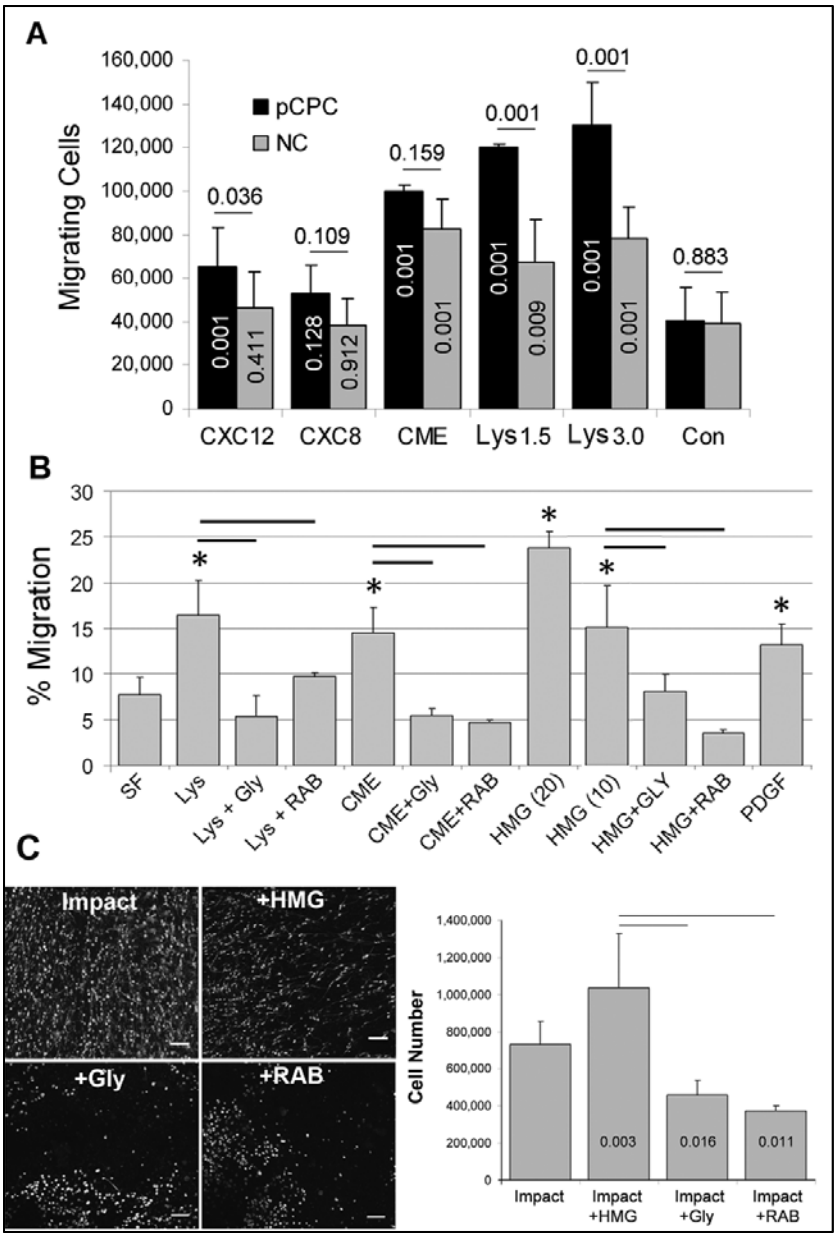

Figure 4. Chemotactic activity of CPCs. (A) The columns show numbers of cells that responded to CXCL12, CXCL8, conditioned medium, (CME), or cell lysates (Lys) made from 1.5 x 10^6 cells (1.5) and 3.0 x 10^6 cells (3.0). or serum-free medium (SF). The numbers above the bars indicate p values for differences between pCPC and NC. Numbers within columns are p values for differences between treatments and SF. (B) Effects of glycyrrhizin (Gly) and anti-RAGE antibody (RAB) on responses to CME, Lys (3.0 x 10^6 cells), and HMGB1 [HMG (10)= 10 nM, HMG (20) =20 nM] on pCPC chemotaxis (% Migration). Columns and error bars are means and standard deviations (n = 3-9). Asterisks indicate p values of less than 0.005 for treated versus SF (one-way ANOVA). (C) Confocal images show results for an untreated impacted control (Impact) and for impacted explants treated with HMGB1 (+HMG), glycyrrhizin (+Gly), and anti-RAGE antibody (RAB). Bars = 100 □m. The histogram on the right shows means and standard deviations for yields of migrating cells (n=4/group). p values (versus Impact-only) are indicated in the columns. Horizontal bars show significant differences between the HMG-treated and Gly-treated groups and between the HMG-treated and RAB-treated groups (p = 0.001).

2.4 Animal models of injury

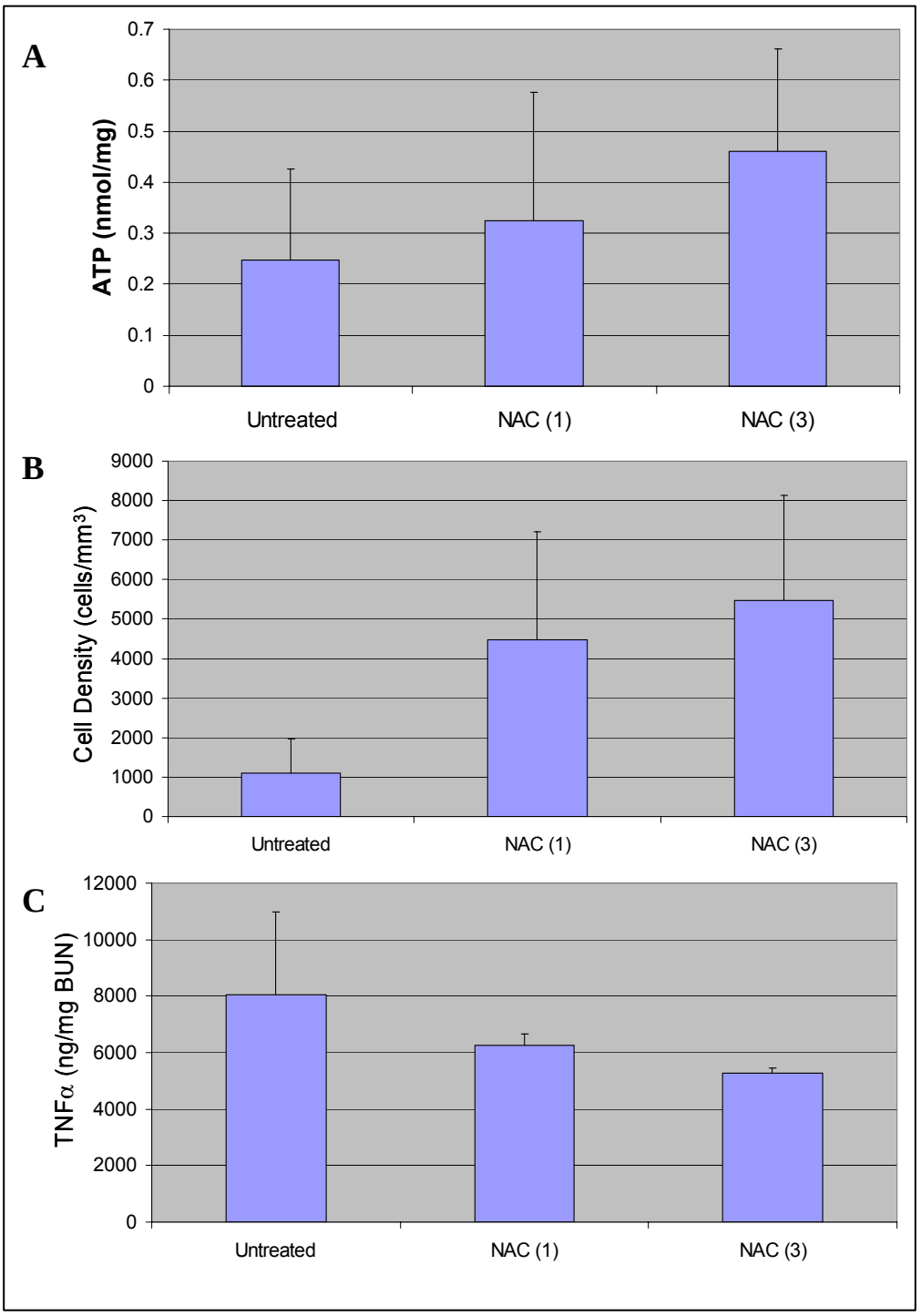

Figure 5. Effects of n-acetyl cysteine (NAC) treatment in a rabbit model. The data show analyses of rabbit cartilage and serum (n=4) 1 week after a single blunt impact injury to the medial femoral condyle. (A) ATP of cartilage from the impact site in untreated animals and animals treated with NAC once immediately after impact (NAC 1) or three times (NAC 3) (immediate, 6 and 24 hours post-impact). (B) Viable cell density at the impact site (C) Tumor necrosis factor alpha (TNFα) in serum.

Very fortunately, a number of drugs capable of breaking the alarmin-chemokine-synovitis response are available for testing. For example, using a rabbit stifle blunt impact model we are currently running tests of n-acetyl cysteine (NAC), an agent that reduces alarmin release by reducing chondrocyte death rates. Encouraging results were seen in a recent pilot study summarized in **Figure 5**. In the near future we plan to test glycyrrhizin, a natural product that chelates HMGB1, effectively blocking CPC activation. These studies will help to determine if on balance CPCs activities are beneficial or harmful.

2.4 Patient studies

In addition to work the in vivo model described above, we are pursuing patient studies aimed at estimating the alarmin/chemokine burden in synovial fluids and effusions drawn at the time of injury and weeks later at the time of surgery **(Figure 6)**. As the alarmin hypothesis applies to any insult that results in extensive intra-articular cell death, we plan to follow a broad range of injuries including intra-articular fractures of the ankle and ligamentous injuries in the knee. A joint fluid repository has been established in the Orthopaedic Biology Laboratory to facilitate these studies. The study is expected to reveal if alarmin/chemokine levels will correlate with imaging-based estimates of injury severity.

2.5 Novel means to identify resident CPCs

Our thorough molecular characterization of injury-responsive CPCs has enabled us to develop new markers that may be useful for identifying CPCs in cartilage specimens before they migrate to the surface. Previous attempts to distinguish CPCs residing in the matrix from normal chondrocytes based on expression of stem-cell or other markers have not been successful. On the other hand, our findings showed that upon exposure to alarmins, CPCs express a number of genes at levels that were 10-fold or more higher than normal chondrocytes. Based on this we hypothesized that an alarmin "challenge" would stimulate gene over-expression by CPCs resident in the matrix. We are currently testing this idea using immunostaining to localize such gene products (CXCL8 and 12 as well as IL-6) in cartilage at various times after alarmin exposure **(Figure 7)**. If our hypothesis is correct, this technique will definitively determine the origins of CPCs. Moreover, we expect that the challenge approach could be used to assay for CPCs in cartilage samples from people of various ages to determine if their numbers decline with age.

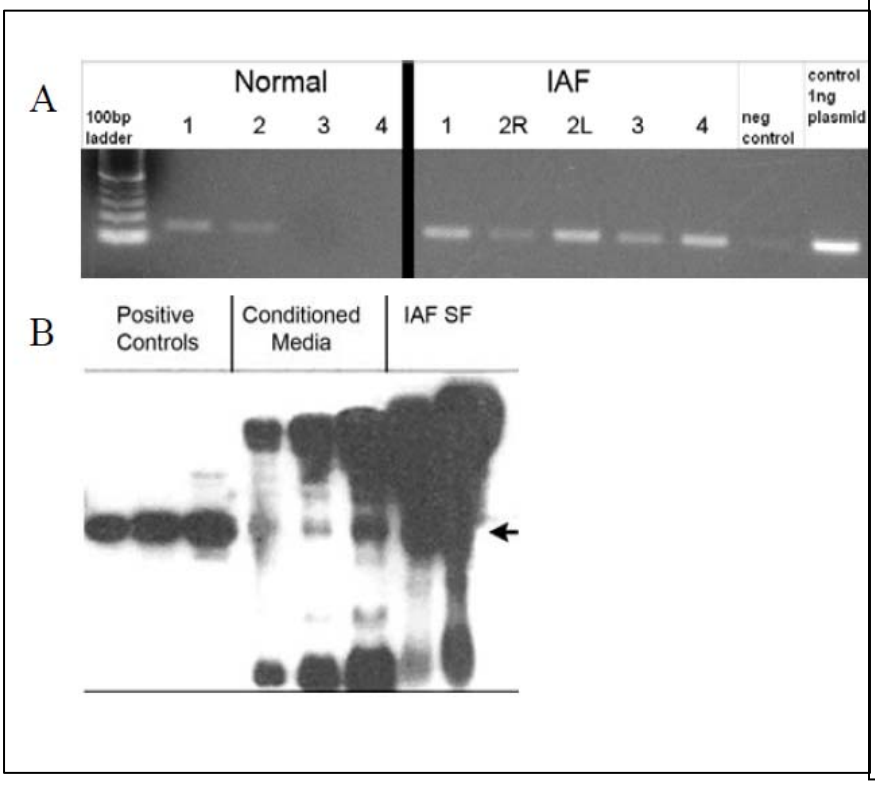

Figure 6. Alarmin levels increase in response to injury. (A) PCR products resulting from amplification of mitochondrial DNA in synovial fluids from 4 normal ankles and from 4 fractured ankles (IAF). 2R and 2L refer to samples collected from the patient's fractured ankle (L) and the contralateral uninjured ankle (R). (B) Western blot for HMGB1 shows results for conditioned medium from an injured explant and synovial fluid from a patient with IAF Samples of conditioned medium from impacted explants, human joint fluid from a fractured ankle, and chondrocyte lysates were all positive for HMGB1. Positive controls consisting of Jurkat cell lysates are also shown.

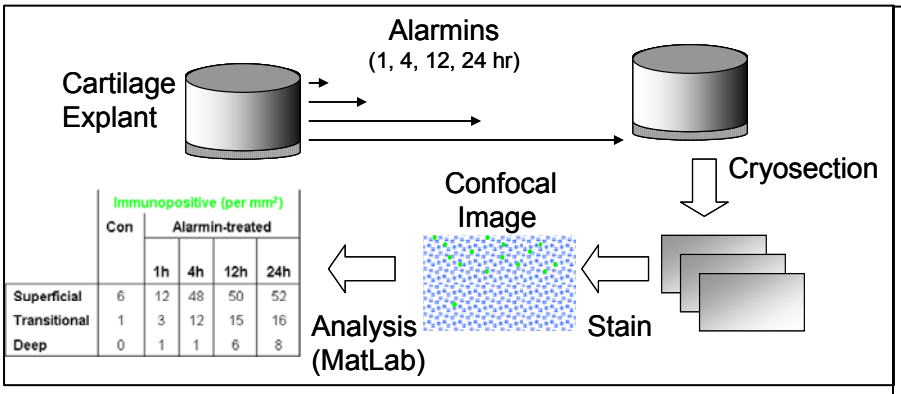

Figure 7. Alarmin challenge to identify and measure resident CPCs in cartilage specimens. Cartilage explants are exposed to alarmins (e.g. HMGB1) that activate high level expression of CXCLs and other genes that are expressed at low levels by normal chondrocytes. An automated MatLab-based image analysis program is used to count positive cells in three cartilage zones.

2.6 Departures from the S.O.W.

In using an explant impact injury model rather than the ex-vivo fracture model our studies departed significantly from the plan described in the SOW. The decision to stay with the explant model was strategic and based on advances that occurred after the SOW was written. First, it became clear that Dr. Tochigi would produce animal models, including rabbit impact and a porcine intra-articular fracture model, sooner than we had expected. The opportunity to skip directly to in vivo systems made the ex vivo fracture model somewhat less attractive as a stepping stone. At the same time we were learning from the explant model about the mechanics of CPC homing and their potential for harm. The findings were so novel and significant that we felt compelled to pursue them to a publishable conclusion.

3. KEY RESEARCH ACCOMPLISHMENTS:

- Identified injury-responsive CPCs in cartilage
- Demonstrated that chondrocyte death stimulates CPC activation
- Alarmins (e.g. HMGB1) are a primary activators and chemoattractants for CPCs
- CPCs invade and re-populate cartilage defects
- CPCs may contribute to post-traumatic inflammation in joints
- New conceptual model linking traumatic cell death and post-traumatic inflammation
- New "alarmin challenge" approach to CPC mapping and counting

4. REPORTABLE OUTCOMES

Manuscript: *Chondrogenic Progenitors Respond to Cartilage Injury*. Seol, D, McCabe D, Choe H, Zheng H, Yu Y, Jang K, Walter M, Lehman A, Ding L, Buckwalter JA, Martin JA. 2012. submitted to Arthritis and Rheumatism

Podium Presentation: *Identification of chondrogenic progenitor cells in injured bovine cartilage*. Y. Yu, D. Seol, D. McCabe, H. Zheng, J. Martin. September 2011, OARSI World Congress on Osteoarthritis, San Diego, CA

Licenses: A quantitative cell imaging program (QCIP) is under review for licensing to MatLab (Mathworks)

Degrees: Dongrim Seol, Ph.D. Biomedical Engineering, University of Iowa 2011. Thesis: *Chondrogenic progenitor cell response to cartilage*

Repository: A repository of joint fluids from patients with intra-articular fracture and ACL injuries has been established in the Orthopaedic Biology Laboratory. The samples will be assayed for alarmins, chemokines and cytokines present in joint fluids in the first few weeks after injury

Funding: We are planning to submit proposals based on this project to the Veterans Administration and Arthritis Foundation. Funding will be used to pursue work in animal models.

5. CONCLUSION: Our results to date have broken new ground with respect to understanding how CPCs function in articular cartilage injuries. While the data show there is a potential for CPC-based cartilage repair, our new findings that implicate CPCs in acute post-traumatic inflammation challenge conventional wisdom that progenitor cells should benefit healing. In addition, our gene expression data have equipped us with new methods for distinguishing CPCs from normal chondrocytes, which will be particularly useful for studying aging effects on CPC populations and for identifying CPCs in the complex milieu of the living joint. The discovery of the role of HMGB1 as a major CPC activator and chemotactic factor provides a means to manipulate the cells to either block or enhance their activation. Hence we are now in an excellent position to test hypotheses regarding the effects of CPC in *in vivo* models of joint injury where interactions with the immune system will be of particular interest.

APPENDIX

Chondrogenic Progenitor Cells Respond to Cartilage Injury

Dongrim Seol, Ph.D.[1,§], Daniel J. McCabe, B.S.[1,§], Hyeonghun Choe, M.E.[1,2], Hongjun Zheng, Ph.D.[1], Yin Yu, B.M.[1,2], Keewoong Jang, M.S.[1,2], Morgan W. Walter, B.S.[1], Abigail D. Lehman, B.S.[1], Lei Ding, Ph.D.[1], Joseph A. Buckwalter, M.D.[1,3], James A. Martin, Ph.D.[1,*]

[§]Both authors contributed equally to this work.

Institutions:

[1]Department of Orthopaedics and Rehabilitation, The University of Iowa, Iowa City, IA

[2]Department of Biomedical Engineering, The University of Iowa, Iowa City, IA

[3]Veterans Affairs Medical Center, Iowa City, IA

Corresponding Author:

James A. Martin, PhD; Address: 1182 Medical Laboratories, The University of Iowa, Iowa City, IA 52242; Tel.: 319-335-7550; Fax: 319-335-7968; E-mail address: james-martin@uiowa.edu

Acknowledgements: This work was supported by the Department of Defense (W81XWH-10-1-0702a) and by a grant from the World Arthrosis Organization. The authors thank Dr. Tae-Hong Lim for his hydrogel formulation, Dr. Prem S. Ramakrishnan for developing a cartilage dissection jig, and Mr. Sean M. Martin for his indispensible help with migration assays.

Running Head: Chondrogenic Progenitor Cells and Cartilage Injury

Abstract

Objective: Hypocellularity resulting from chondrocyte death in the aftermath of mechanical injury is thought to contribute to post-traumatic osteoarthritis. However, we found that nonviable areas in cartilage injured by blunt impact were repopulated within 7-14 days by cells that appeared to migrate from the surrounding matrix. We hypothesized that the migrating population included chondrogenic progenitor cells drawn to injured cartilage by alarmins.

Methods: Osteochondral explants from mature cattle were injured by blunt impact or scratching, resulting in localized chondrocyte death. Injured sites were serially imaged by confocal microscopy and migrating cells were evaluated for chondrogenic progenitor characteristics. Chemotaxis assays were used to measure the responses to chemokines, injury-conditioned media, dead cell debris, high mobility group box 1 (HMGB1).

Results: Migrating cells were highly clonogenic, multipotent, and expressed markers associated with chondrogenic progenitors. Compared with chondrocytes, these cells over-expressed genes involved in proliferation and migration, and under-expressed cartilage matrix genes. They were more active in chemotaxis assays than chondrocytes and responded to cell lysates, conditioned medium, and HMGB1. Glycyrrhizin, a chelator of HMGB1 and a blocking antibody to the receptor for advanced glycation end products (RAGE) inhibited responses to cell debris and conditioned medium, and reduced the numbers of migrating cells on injured explants.

Conclusion: Injuries that caused chondrocyte death stimulated the emergence and homing of chondrogenic progenitors in part *via* HMGB1 release and RAGE-mediated chemotaxis. Their repopulation of the matrix could promote the repair of chondral damage that might otherwise contribute to progressive cartilage loss.

Introduction

The risk for post-traumatic osteoarthritis (PTOA) after serious joint injuries still runs as high as 70% despite many refinements in care (1-3). This underscores the urgent need for new treatments to prevent articular cartilage loss initiated by joint damage and cartilage injury. Most macroscopic cartilage lesions don't heal and may spread locally or stimulate joint-wide cartilage degeneration (1, 4). This occurs despite the presence of

potentially reparative chondrogenic progenitor cells (CPCs) in cartilage and other intra-articular tissues (5-8) which show vigorous *in vitro* chondrogenic activity. It may be possible to coax these cells to be more effective *in vivo*, but more complete knowledge of the post-traumatic behavior and function of CPCs is needed to evaluate this potential.

Like mesenchymal stem cells (MSCs) that originate in bone marrow, progenitor cells residing in tissues are multipotent, highly clonogenic, and chemotactic (9-11). Progenitor cells migrate locally to sites of injury where they proliferate and differentiate as needed to replace damaged tissue (12, 13). Unlike MSCs, which must be capable of differentiating suitably for the regeneration of multiple tissues in different organ systems, local tissue regeneration by progenitors does not require such pluripotency and the progenitor cells' repertoire is typically more limited than that of MSCs (12).

CPCs were first identified in calf cartilage as a sub-population of superficial zone cells required for the appositional growth of articular cartilage (5, 14). The specialized population was isolated from other cartilage cells based on enhanced binding to fibronectin. Compared with normal chondrocytes (NCs), CPCs over-expressed the stem cell-associated factor Notch-1 and the fibronectin receptor α5β1 integrin. The cells also showed enhanced clonality in culture and multi-potency when grafted to chick limb buds. Alsalameh and co-authors subsequently showed that approximately 4% of the cells in normal human cartilage expressed the mesenchymal stem cell markers CD105 and CD166 (15). This frequency increased to near 8% in osteoarthritic cartilage. However, less than half of the CD105+/CD166+ cells were capable of adipogenic differentiation, suggesting that CD marker status overestimated the numbers of multipotent MSC-like progenitors. Using fluorescent activated cell sorting analysis, Hattori *et al*. demonstrated that 0.07% of the cells present in the superficial zone of calf stifle cartilage were capable of Hoechst 33342 dye exclusion, whereas none of the cells from the middle or deep zones excluded the dye (7). As expression of the multi-drug transporter responsible for dye exclusion is typical of stem cells, the authors concluded they had found a stem-like progenitor cell population (16). A sub-population of CD13-, CD29-, CD44-, CD73-, CD90-, and CD105-expressing cells were found in repair tissue in osteoarthritic cartilage obtained at the time of total joint replacement. The cells appeared to migrate from subchondral bone *via* tidemark-spanning blood vessels and expressed both the

osteoblastic transcription factor Runx-2 and the chondrogenic transcription factor Sox-9 (8, 17). Concurrently, Grogan and coworkers found high numbers of chondrocytes (>45%) that were immunohistologically positive for the MSC markers Notch-1 and Stro-1 in both normal and osteoarthritic cartilage (6). These cells were osteogenic and chondrogenic, but not adipogenic. They included a small side population of Hoechst dye-excluding cells (0.14%).

Necrotic cell death associated with wounding releases intracellular components that serve as chemotactic signals for progenitor and stem cells, and leukocytes. Known collectively as "alarmins" or danger-associated molecular patterns (DAMPs) they include mitochondrial DNA and formyl methionine (fMet) containing peptides and DNA-binding high mobility group proteins such as HMGB1 and 2, and multiple S100 proteins (18-21). Alarmin binding to RAGE and toll-like receptors (TLRs) stimulates the migration of progenitor and stem cells, attracting them to injury sites where they participate in tissue regeneration and repair (22-25). The potent anti-inflammatory drug glycyrrhizic acid is a natural product derived from licorice that binds HMGB1 and blocks its activities (26). Additional chemotactic recruitment is stimulated by C-X-C motif ligands (CXCL) released by tissue and inflammatory cells (27, 28). A number of studies have shown that blunt trauma to articular cartilage induces acute chondrocyte necrosis and apoptosis (1, 29-35). In an explant trauma model we found cells migrating over cartilage surfaces near sites of extensive chondrocyte death. These cells were isolated and evaluated for progenitor characteristics and chemotactic responses to injury-related alarmins.

Materials and Methods

Bovine stifle joints from young adult cattle (15-24 months-old) were obtained from a local abattoir (Bud's Custom Meats, Riverside, IA). Osteochondral explants were prepared by manually sawing an approximately 25 x 25 mm^2 from bovine tibial plateau, which included the central loaded area of the articular surface. Osteochondral explants were prepared in the same manner from three normal human tali harvested under IRB approval from patients undergoing lower limb amputation for cancer. The patients were males aged 29, 34, and 46 years and were not diagnosed with osteoarthritis. The explants were rinsed in Hanks Balances Salt Solution (HBSS) and cultured in Dulbecco's modified Eagle medium (DMEM) supplemented with 10%

fetal bovine serum (Invitrogen™ Life Technologies, Carlsbad, CA), 50 μg/ml L-ascorbate, 100 U/ml penicillin, 100 μg/ml streptomycin, and 2.5 μg/ml Fungizone.

After two days in culture the human and bovine explants were injured by blunt impact (14 J/cm^2) *via* a 5 mm-diameter flat-ended platen using a drop tower device as described previously (35, 36). In some cases explant cartilage was dissected free from subchondral bone immediately after impact injury. Scratch injuries were made by dragging a 26 gauge needle over the cartilage surface to create X-shaped matrix tears ~ 0.5 mm in depth. Confocal imaging studies were performed essentially as described (35, 36). Briefly, explants were stained with calcein AM (viability) and ethidium homodimer (dead cells) and submerged in culture medium. After a 30-minute incubation the explants were imaged using a Bio-Rad 1024 laser scanning confocal microscope (LSCM) (Bio-Rad Laboratories Inc., Hercules, CA).

Five to seven days post-injury explants were submerged in 0.25% trypsin-EDTA in HBSS and were incubated for 10 minutes to detach migrating progenitor cells from the surface. Pre-and post-trypsin imaging studies confirmed that the brief enzymatic treatment removed the surface-adherent migrating cells without disrupting the underlying superficial chondrocytes. To recover normal chondrocytes the underlying cartilage was digested overnight with collagenase type 1 and pronase E (Sigma-Aldrich, St. Louis, MO) dissolved in culture medium (0.25 mg/ml each). A custom-fabricated device was used to separate the superficial 1/3 and lower 2/3 of the cartilage samples zones prior to collagenase/pronase digestion. Colony forming assays were performed as previously described (37).

For some experiments isolated pCPCs cells were labeled with Green Fluorescent Protein (GFP, 488 nm) by lentiviral transduction. GFP-labeled cells (1x10^5) were suspended in a chilled (8°C) hydrogel consisting of 0.6% 2KDa hyaluronic acid (Easy Motion Horse, Niagara Falls, NY) and 18% Pluronic F-127 (Sigma-Aldrich) in normal saline. Pluronic F-127 is a polyol surfactant that confers temperature-sensitive gelation to solutions (38). The cold suspension gelled on contact with warmed (37°C) explants, such that the suspended cells were held in place adjacent to a blunt impact site. The explants were incubated for 5 days when they were counterstained with 0.5 μM Cell Tracker Red CMTPX (Invitrogen™ Life Technologies) and imaged on a Bio-Rad 1024 confocal microscope with the custom-built x-y microscope stage driver (CMSD). The sites were

scanned to an average depth of 330 μm at 40 μm intervals. Z-axis projections of confocal images were made using ImageJ (rsb.info.nih.gov/ij).

Immunofluorescence staining for proliferating cell nuclear antigen (PCNA) was performed on paraformaldehyde-fixed cryosections of cartilage from three different explants that had been cultured for 10 days after an impact injury using a monoclonal anti-PCNA antibody (Abcam, Cambridge, MA) and a goat anti-mouse fluorescent secondary antibody (Alexafluor 488) from Jackson Immunoresearch (West Grove, PA) was used for detection. The sections were mounted in Vectashield with DAPI (Vector Labs, Burlingame, CA) to stain nuclei. Additional sections from the same explants stained with safranin-O/fast green to reveal tissue morphology. PRG4 (lubricin) immunohistochemistry was performed on sections from the same specimens with a mouse monoclonal antibody (MD Biosciences, St. Paul, MN) and a Vectastain ABC detection kit (Vector Labs). Transmitted light and epifluorescence images were taken on a Qimage CCD camera (Qimaging, BC, Canada) mounted on an Olympus BX60 microscope.

Cell migration/chemotaxis assays were performed using CytoSelect™ 24-Well Cell Invasion Assay kit (Cell Biolabs Inc., San Diego, CA) essentially as described by the manufacturer. pCPC or NC suspensions ($3x10^5$ cells in serum-free medium) were added to the upper transwell and placed in reservoirs containing serum-free medium alone or serum-free medium with various chemokines, cell lysates, or serum-free medium conditioned by injured explants. The plates were incubated for 24 hours, prior to processing. Cell lysates were transferred to fluorescence plates and read on a microplate reader (Molecular Devices Inc., Sunnyvale, CA). The data are presented as the percentage of migrating cells (# in the bottom chamber / # seeded x 100). Conditioned medium was made by incubating blunt-impacted explants overnight in 10 ml serum-free medium. The medium was concentrated 10-fold using Amicon® Ultra centrifugal Filters 10K (Millipore, Billerica, MA). Lysates for testing in the chemotaxis assay were obtained by repeated freeze-thawing of cells from primary cultures of bovine chondrocytes isolated from distal femurs. Glycyrrhizic acid (Sigma-Aldrich) and a rabbit polyclonal anti-RAGE antibody (Abcam) were added to culture media at a concentration of 25 μM (39). Porcine platelet-derived growth factor (PDGF-BB) (R&D Systems, Minneapolis, MN) was diluted in medium to a concentration of 300 nM (40). The effects of glycyrrhizic acid and anti-RAGE antibody on migration in the

explant model were assessed by confocal microscopy and by counting migrating cells harvested from explant surfaces by trypsinization at 14 days post-impact. The explants (n = 4/group) were treated daily starting immediately after impact.

Side population assays were performed essentially as described (7). First passage pCPCs and NCs in suspension in HBSS ($1x10^6$/ml) were incubated at 37°C for 1.5 hours with Hoechst-33342 (Sigma-Aldrich) at 2.5 mg/ml with or without verapamil (Sigma-Aldrich) at 5 mM. The cells were washed in cold HBSS, filtered through 70 μm nylon mesh and counterstained with propidium iodide to identify dead cells. Flow cytometric analysis was performed on a Becton Dickinson LSR II with UV (BD Bioscience, San Jose, CA).

The multi-potency of pCPCs was tested by culturing them under chondrogenic, osteogenic and adipogenic conditions (41). For chondrogenic differentiation, 1.2 million cells were pelleted and incubated in chondrogenic medium (DMEM containing 10 ng/ml TGF-β1, 0.1 μM dexamethasone, 25 μg/ml L-ascorbate, 100 μg/ml pyruvate, 50 mg/ml ITS+Premix and antibiotics) for 14 days. The pellets were analyzed for matrix formation using Safranin-O/fast green staining of cryosections. To induce osteogenic differentiation, $3x10^4$ trypsinized migrating cells were cultured in osteogenic medium (DMEM/F-12 containing 0.1 μM dexamethasone, 100 mM β-glycerophosphate, 50 μg/ml L-ascorbate and antibiotics) for 14 days and stained with Alizarin Red to detect deposition of calcium phosphate mineralization. We used STEMPRO® Adipogenesis differentiation kit (GIBCO, Grand Island, NY) to induce adipogenesis. Fourteen days post-induction, the cells were stained with Oil Red O and imaged on a Nikon XB inverted microscope.

For microarray analysis we isolated RNA from primary cultures of bovine MSCs, from freshly harvested pCPCs, and directly from explant cartilage. MSCs were isolated from the marrow and subchondral bone of adult bovine tibiae by saline lavage. The lavage was centrifuged and the pelleted cells plated in plastic dishes. Adherent cells were cultured for 5 days before harvest. RNA was harvested from three independent batches of cells/explants. Cells and cartilage were homogenized in TRIzol® reagent (Invitrogen™ Life Technologies) and total RNA was extracted using the RNeasy Mini Kit (Qiagen, Valencia, CA) according to the manufacturer's instructions. RNA (50 ng) was converted to SPIA amplified cDNA using the Ovation™ RNA Amplification System v2 (NuGEN Technologies Inc., San Carlos, CA) Biotinylated cDNA was placed onto

Bovine Genome Arrays (Affymetrix Inc., San Carlos, CA). Arrays were scanned with the Affymetrix Model 3000 and data were collected using the GeneChip operating software (MAS) v5.0. Statistical analysis of the data (one-way ANOVA) and a heatmap and dendrogram were generated using Partek Genomics Suite software (Partek, St. Louis, MO).

Previously published work indicated that progenitor cells can be distinguished from normal chondrocytes based on up-regulation of genes expressed in mesenchymal stem cell populations (5, 6). These genes include the ATP-binding cassette sub-family G member 2 (ABCG2), various cluster of differentiation (CD) markers, fetal liver kinase-1 (FLK-1), runt-related transcription factor 2 (Runx-2), and sex determining region Y-box 9 (Sox-9). Beta actin was used for normalization. Real-time PCR was used to compare the expression of these markers in pCPCs and NCs essentially as described (42). Primers were purchased from Integrated DNA Technologies (Coralville, IA). The following primer sequences were used (Forward/Reverse):

1) ABCG2; CCTTGGTTGTCATGGCTTCA/AGTCCTGGGCAGAAGTTTTGTC

2) CD105; CCACTGCCCCAGAGACTGCGC/GCCCCCACAGTGAGTGCTTAGGT

3) CD90; CGGTGGTGTTTGGCCATGTAATGA/GAGAGAGGGGAGTCCTATCCTGGT

4) CD73; AGCTTTCCCAGCCTTCCATGCG/GGGTGTCCTCTTGAGTCCTGCA

5) CD39; CCCACCCTCTCCTTCCGAGAGG/TGACTGTAACCCTGGAGCTTGGCT

6) CD29; GCGGCCTCCGGGTGGATTCC/GCCGGGAAGGTCCAGGGGC

7) FLK-1; TTCCAAGTGGCTAAGGGCAT/TTTAACCACGTTCTTTTCCGACA

8) Runx-2; GCATGAAGCCCTATCCAGAGTCT/GCTGATGGAGCTGTTGGTGTAG

9) Sox-9; CGGTGGTGTTTGGCCATGTAATGA/GAGAGAGGGGAGTCCTATCCTGGT

10) b-actin; TCGACACCGCAACCAGTTCGC/CATGCCGGAGCCGTTGTCGA

For colony formation assays statistical analysis was performed using SPSS software (Ver.10.0.7, SPSS Inc., Chicago, IL) with a one-way ANOVA and post-hoc pairwise comparison. Flow cytometry data (side

population) were evaluated by Students t-test. One-way and Two-way ANOVAs with the Holm-Sidak post-hoc test were used to analyze migration assay data. All the results are expressed as mean ± standard deviation.

Results

Blunt impact-injury to explant surfaces caused local chondrocyte death and stimulated the emergence of migratory cells in and around impact sites. These cells began to accumulate 5 days after impact and gradually repopulated previously uninhabited areas (Figure 1A-C). Migrating cells were morphologically distinct from NCs in that they were elongated with multiple thin cytoplasmic extensions (Figure 1D). A similar migratory reaction was observed at impact sites in explanted human tali, one of which is shown (Figure 1E and F) and in a scratch injury (Figure 1G and H). Migrating cells were also observed on impacted explant cartilage cultured without subchondral bone. A specimen representative of three such explants is shown (Figure 1I). Immunostaining of cryosections from impacted explants revealed that surface-migrating pCPCs were positive for PCNA, whereas chondrocytes beneath the surface were largely negative (Figure 1J). Surface pCPCs were also strongly positive for lubricin (Figure 1K).

After 5-7 days post-impact surface-adherent migrating cells were detached from the injured explants by trypsin treatment. Some cells were transduced with GFP, and grafted ~4 mm away from a freshly made impact site on another explant (Figure 2A). The number of labeled cells in the impact site increased dramatically from 2-12 days (Figure 2B-D). The clonogenic activity of trypsinized cells was compared with chondrocytes from the upper 1/3 of the cartilage, which included the superficial and transitional zones, and from the bottom 2/3, which included the transitional and deep zones (Figure 3). Primary cultures were established and the cells harvested for colony formation assays after 5-7 days in culture. Trypsinized cells in monolayer culture grew more rapidly in primary cultures than chondrocytes (Figure 3A-D). These cultures were passaged, seeded in cloning dishes and incubated for 10 days. Trypsinized cells showed the most vigorous colony formation both in terms of the total number of colonies and average colony size (Figure 3E, F and G). Trypsinized cells and chondrocytes from the upper 1/3 of the cartilage matrix showed significantly higher numbers of colonies (150 and 120 respectively) than chondrocytes from the bottom 2/3 of the matrix (20 colonies) ($p = 0.001$). The average colony size for trypsinized cells of 20 mm^2 was significantly greater than for chondrocytes from the upper 1/3

or lower 2/3 of the matrix, which both showed averages of less than 5 mm^2 ($p = 0.001$). However, ~1% of the colonies formed by upper 1/3 chondrocytes showed areas of 20 mm^2 or greater.

pCPCs were cultured in chondrogenic, osteogenic, or adipogenic media for 14 days to evaluate their differentiation potential. After the induction of chondrogenic differentiation, cultured pellets were fixed and stained with Safranin-O/fast green, revealing a proteoglycan-rich matrix throughout the pellets (Figure 4A). Similarly, most cells in osteogenic medium deposited a calcium phosphate-rich mineralized matrix as detected by Alizarin Red staining (Figure 4B). However, few cells (< 1%) stained with Oil Red O after 2 weeks of culture in adipogenic medium (Figure 4C).

Flow cytometric analysis of Hoechst-stained NCs revealed few side population cells (0.032 +/- 0.012%) (Figure 4D). The side population was significantly larger in trypsinized cells (0.22 +/- 0.07%, $p=0.001$). Verapamil treatment reduced side populations to less than 0.005%, indicating that stain efflux depended on the stem cell-associated ABCG2 transporter. Real-time PCR analysis revealed substantially higher expression of stem cell marker genes in pCPCs versus NCs (Figure 4E). ABCG2 was increased by over 4-fold, Sox-9 by 3.8-fold, and FLK-1 by 2.8-fold. CD105, CD73, CD39, and CD29 were increased by less than 2-fold in pCPCs and CD90 was 2-fold higher in NCs than in pCPCs. Microarray analysis showed elevated expression of the progenitor cell markers Notch1 (7.4-fold) and CD44 (12-fold) in pCPCs compared to NCs.

Statistical analysis of microarrays indicated that overall gene expression in pCPCs was more similar to that of MSCs than NCs (Figure 4F). Individual genes that showed statistically significant differences in expression ($p<0.05$) of greater than 2-fold in pCPCs *versus* NCs or MSCs are listed (Table). The listed genes were selected for relevance to inflammation, proliferation, migration, and chondrogenic differentiation. The pro-inflammatory cytokine IL-6 was among the most highly up-regulated genes in CPCs compared with NCs (130-fold increase). Chemokines involved in stem cell and leukocyte chemotaxis (28, 43) were also strikingly up-regulated in pCPCs relative to NCs: CXCL12 expression was more than 25 times greater and CXCL8 (IL8) increased by more than 35-fold. Also relative to NCs, the matrix metalloproteinases, MMP1 and MMP13, were over-expressed in pCPCs by 18- and 4.3-fold respectively and the proliferation-related cyclins B1 (CCNB1) and D1 (CCND1) were over-expressed by 35- and 9-fold respectively. Relative to NCs, genes encoding the

cartilage extracellular matrix components collagen type X (COL10A1), type IX (COL9A2), and type II (COL2A1), aggrecan (ACAN), and cartilage oligomeric matrix protein (COMP) were among the most down-regulated genes in pCPCs. However, *versus* MSCs, pCPCs over-expressed the superficial chondrocyte marker PRG4 (proteoglycan-4/lubricin), and the chondrocyte-associated genes S100A1 (16-fold) and S100B (2.6-fold). Moreover, ACAN and COL2A1 expression was much higher in pCPCs than in MSCs (17 and 6.9-fold increases respectively). In contrast, the gene for the interleukin 1 receptor antagonist (IL1RN) was substantially down-regulated in pCPCs versus MSCs (-3.6-fold), as were several insulin-like growth factor binding proteins including IGFBP7 (-10-fold), IGFBP3 (-5.4-fold), and IGFBP2 (-3.6-fold).

In general, pCPCs were significantly more active in transwell chemotaxis assays than NCs (p=0.001), however this was factor-dependent (Figure 5A). Compared with untreated control medium, CXCL12 significantly increased pCPC chemotaxis (p=0.001), but had no effect on NCs (p=0.411). Neither pCPCs nor NCs responded to CXCL8 (p=0.128 and 0.912 respectively), but conditioned medium from impact-injured explants induced chemotaxis to a similar degree in both pCPCs and NCs (p=0.001). The response to cell lysates was significant for pCPCs and NCs (p=0.001), but the pCPC response was significantly greater than the NC response (p=0.001). In addition to cell lysates and conditioned medium, pCPCs responded strongly to purified HMGB1 (Figure 5B). HMGB1 at 10 or 20 nM significantly enhanced chemotaxis compared with controls (p=0.001). The stimulatory effects of 10 nM HMGB1 and the effects of conditioned media and cell lysates were significantly suppressed by glycyrrhizin and by an antibody to the AGE receptor (p=0.001). The migratory activity stimulated by lysates, conditioned medium and 10 nM HMGB1 were similar to the activity stimulated by PDGF (250 nM), a well-known stem cell chemotactic factor. Glycyrrhizin and the anti-RAGE antibody also significantly inhibited pCPC migration in impacted explants (p = 0.016 and 0.011 respectively) (Figure 5C).

Discussion

The results of these experiments demonstrate that the migrating cells we observed on injured bovine osteochondral explants closely resembled chondrogenic progenitors previously identified in normal and osteoarthritic human cartilage. The cells' chemotactic activity, clonogenicity, limited multipotency, and side

population were all notably consistent with published descriptions of progenitor cells from cartilage and other tissues (6, 8, 14, 15, 17).

In vitro chemotaxis assays confirmed that medium conditioned by impacted cartilage or cell lysates were relatively strong chemoattractants for pCPCs. Furthermore, a scratch injury that caused localized chondrocyte death much like that observed in impact sites provoked the same response as impact injury, indicating that chondrocyte death was the main cause of pCPC activation in this system. The strong blocking effects of glycyrrhizin in the migration assays implicated the nuclear protein HMGB1 as a primary chemoattractant in these complex mixtures. A blocking antibody to the RAGE receptor also significantly diminished migration, indicating that HMGB1 effects were mediated in part by RAGE. The inhibitory effects of glycyrrhizin and anti-RAGE on pCPC migration/proliferation in the explant system were also significant; however, the treatments were less potent than in transwell migration assays, suggesting that other factors contributed to the chemotactic activity. Indeed, our data suggest that PDGF might play such a role. A similar migratory response was observed in explanted human tali with the same impact injuries as bovine explants, indicating that pCPC activation was not unique to the bovine system.

pCPCs appeared after injury when cartilage was cultured separately from subchondral bone. Cell populations derived from the top 1/3 of the cartilage matrix consistently yielded a few colonies that were as large as those formed by pCPCs, whereas cells from the bottom 2/3 of the matrix never formed such colonies. Moreover, PRG4, which is expressed at high levels by superficial chondrocytes, was one of the most highly up-regulated genes in pCPCs relative to MSCs. These findings strongly suggest that pCPCs resided in the superficial zone before cartilage injury.

Compared with NCs, pCPCs over-expressed a few, but not all stem cell-associated markers; while ABCG2, Runx2, and Notch1 expression were up by 4-fold or more in pCPCs, increases in CD markers were minor (< 2-fold) and not likely to be biologically significant. These results mainly agree with previous work (5, 7, 15, 17), but the lack of substantive increases in CD marker expression suggests the pCPCs studied here might differ from progenitors of sub-chondral origin that more clearly over-express these markers (17). Relative to NCs, CPCs under-expressed chondrocyte-associated genes such as COL2A1 and ACAN. However, compared

with MSCs, pCPCs over-expressed COL2A1, ACAN, PRG4, S100A1, and S100B, all of which are considered to be chondrocyte markers (44). Thus, although they more closely resembled MSCs in their overall pattern of gene expression, pCPCs retained some chondrocyte-like features and were distinguishable from MSCs on that basis.

The expression of several matrix proteases (MMP1, MMP13, ADAMTS4, ADAM8, and ADAM9) was significantly higher in pCPCs than in NCs. This was consistent with the enhanced chemotactic activity of pCPCs compared with NCs in our transwell-based assays, which measured movement through a collagen matrix. With the notable exceptions of MMP1 and MMP13, which were upregulated by more than 4-fold in pCPCs, matrix proteases were expressed at similar levels by MSCs, whose physiologic functions include migration through extracellular matrices.

The accumulation of hundreds of pCPCs at injury sites was unlikely to be due solely to migration from the surrounding matrix. pCPCs grew rapidly in culture and proliferation on cartilage surfaces is likely to explain the rapid repopulation of impact sites in the explant model. This was corroborated by immunofluorescence staining, which identified relatively high numbers of PCNA-positives among surface migrating cells. Consistent with their highly clonogenic, proliferative phenotype, both MSCs and pCPCs significantly over-expressed CSF (colony stimulating factor), cyclins, and other growth-related genes.

The circumstances of the explant experiment dictated that we use different techniques to harvest RNA from CPCs and NCs: CPC RNA was from cells freshly removed from explant surfaces by trypsinization and NC RNA was extracted directly from cartilage and MSC RNA was from primary monolayer cultures. Although the trypsin treatment of CPCs was brief (~10 minutes), it might have led to changes in the expression of some early response genes. Moreover, procedural losses associated with RNA extraction from cartilage might have contributed to variability among the NC samples, which was higher than in pCPC or MSC samples. Lastly, the effects of isolation and short-term culture on MSC gene expression are unknown and might have affected many of the genes that appeared to be differentially regulated versus pCPC and NC.

The physiologic functions of CPCs and their effects on healing in injured joints remain unknown. Although CPCs efficiently re-populated damaged cartilage in our model, their relatively high levels of

chemokine and cytokine expression and excessive matrix protease production could contribute to synovitis and cartilage degeneration in injured joints. On the other hand, CPCs may be involved in the early stages of cartilage repair: confocal studies and histology showed that pCPCs formed a continuous sheet over injured cartilage surfaces after a week or more in culture. The relatively high level of PRG4 expression by CPCs observed at the RNA and protein levels suggests they help to restore the surface-protective lubricant coating on damaged cartilage, a process that may be involved in the repair of superficial defects (1, 45-49). The identification of HMGB1 as an activator suggests a method to control CPC responses to promote healing. Whether the goal should be to thwart or augment these responses will likely be decided by findings from *in vivo* models, where treatments can be evaluated in a more physiologic setting.

References

1. Buckwalter JA, Brown TD. Joint injury, repair, and remodeling: roles in post-traumatic osteoarthritis. Clin Orthop Relat Res 2004(423):7-16.
2. Marsh JL, Borrelli J, Jr., Dirschl DR, Sirkin MS. Fractures of the tibial plafond. Instr Course Lect 2007;56:331-52.
3. Marsh JL, Weigel DP, Dirschl DR. Tibial plafond fractures. How do these ankles function over time? J Bone Joint Surg Am 2003;85-A(2):287-95.
4. Hunziker EB. The elusive path to cartilage regeneration. Adv Mater 2009;21(32-33):3419-24.
5. Dowthwaite GP, Bishop JC, Redman SN, Khan IM, Rooney P, Evans DJ, et al. The surface of articular cartilage contains a progenitor cell population. J Cell Sci 2004;117(Pt 6):889-97.
6. Grogan SP, Miyaki S, Asahara H, D'Lima DD, Lotz MK. Mesenchymal progenitor cell markers in human articular cartilage: normal distribution and changes in osteoarthritis. Arthritis Res Ther 2009;11(3):R85.
7. Hattori S, Oxford C, Reddi AH. Identification of superficial zone articular chondrocyte stem/progenitor cells. Biochem Biophys Res Commun 2007;358(1):99-103.
8. Khan IM, Williams R, Archer CW. One flew over the progenitor's nest: migratory cells find a home in osteoarthritic cartilage. Cell Stem Cell 2009;4(4):282-4.

9. Hilfiker A, Kasper C, Hass R, Haverich A. Mesenchymal stem cells and progenitor cells in connective tissue engineering and regenerative medicine: is there a future for transplantation? Langenbecks Arch Surg;396(4):489-97.
10. Pittenger MF, Mackay AM, Beck SC, Jaiswal RK, Douglas R, Mosca JD, et al. Multilineage potential of adult human mesenchymal stem cells. Science 1999;284(5411):143-7.
11. Prockop DJ. Repair of tissues by adult stem/progenitor cells (MSCs): controversies, myths, and changing paradigms. Mol Ther 2009;17(6):939-46.
12. Quesenberry PJ, Colvin G, Dooner G, Dooner M, Aliotta JM, Johnson K. The stem cell continuum: cell cycle, injury, and phenotype lability. Ann N Y Acad Sci 2007;1106:20-9.
13. Spees JL, Whitney MJ, Sullivan DE, Lasky JA, Laboy M, Ylostalo J, et al. Bone marrow progenitor cells contribute to repair and remodeling of the lung and heart in a rat model of progressive pulmonary hypertension. FASEB J 2008;22(4):1226-36.
14. Williams RJ, 3rd, Harnly HW. Microfracture: indications, technique, and results. Instr Course Lect 2007;56:419-28.
15. Alsalameh S, Amin R, Gemba T, Lotz M. Identification of mesenchymal progenitor cells in normal and osteoarthritic human articular cartilage. Arthritis Rheum 2004;50(5):1522-32.
16. Golebiewska A, Brons NH, Bjerkvig R, Niclou SP. Critical appraisal of the side population assay in stem cell and cancer stem cell research. Cell Stem Cell;8(2):136-47.
17. Koelling S, Kruegel J, Irmer M, Path JR, Sadowski B, Miro X, et al. Migratory chondrogenic progenitor cells from repair tissue during the later stages of human osteoarthritis. Cell Stem Cell 2009;4(4):324-35.
18. Klune JR, Dhupar R, Cardinal J, Billiar TR, Tsung A. HMGB1: endogenous danger signaling. Mol Med 2008;14(7-8):476-84.
19. Zhang Q, O'Hearn S, Kavalukas SL, Barbul A. Role of High Mobility Group Box 1 (HMGB1) in Wound Healing. J Surg Res.
20. Jeannin P, Jaillon S, Delneste Y. Pattern recognition receptors in the immune response against dying cells. Curr Opin Immunol 2008;20(5):530-7.

21. Foell D, Wittkowski H, Roth J. Mechanisms of disease: a 'DAMP' view of inflammatory arthritis. Nat Clin Pract Rheumatol 2007;3(7):382-90.

22. Meng E, Guo Z, Wang H, Jin J, Wang J, Wang H, et al. High mobility group box 1 protein inhibits the proliferation of human mesenchymal stem cells and promotes their migration and differentiation along osteoblastic pathway. Stem Cells Dev 2008;17(4):805-13.

23. Stich S, Loch A, Leinhase I, Neumann K, Kaps C, Sittinger M, et al. Human periosteum-derived progenitor cells express distinct chemokine receptors and migrate upon stimulation with CCL2, CCL25, CXCL8, CXCL12, and CXCL13. Eur J Cell Biol 2008;87(6):365-76.

24. Chavakis E, Urbich C, Dimmeler S. Homing and engraftment of progenitor cells: a prerequisite for cell therapy. J Mol Cell Cardiol 2008;45(4):514-22.

25. Palumbo R, Galvez BG, Pusterla T, De Marchis F, Cossu G, Marcu KB, et al. Cells migrating to sites of tissue damage in response to the danger signal HMGB1 require NF-kappaB activation. J Cell Biol 2007;179(1):33-40.

26. Girard JP. A direct inhibitor of HMGB1 cytokine. Chem Biol 2007;14(4):345-7.

27. Kitaori T, Ito H, Schwarz EM, Tsutsumi R, Yoshitomi H, Oishi S, et al. Stromal cell-derived factor 1/CXCR4 signaling is critical for the recruitment of mesenchymal stem cells to the fracture site during skeletal repair in a mouse model. Arthritis Rheum 2009;60(3):813-23.

28. Kucia M, Jankowski K, Reca R, Wysoczynski M, Bandura L, Allendorf DJ, et al. CXCR4-SDF-1 signalling, locomotion, chemotaxis and adhesion. J Mol Histol 2004;35(3):233-45.

29. Carter DR, Beaupre GS, Wong M, Smith RL, Andriacchi TP, Schurman DJ. The mechanobiology of articular cartilage development and degeneration. Clin Orthop Relat Res 2004(427 Suppl):S69-77.

30. Duda GN, Eilers M, Loh L, Hoffman JE, Kaab M, Schaser K. Chondrocyte death precedes structural damage in blunt impact trauma. Clin Orthop Relat Res 2001(393):302-9.

31. Isaac DI, Meyer EG, Haut RC. Chondrocyte damage and contact pressures following impact on the rabbit tibiofemoral joint. J Biomech Eng 2008;130(4):041018.

32. Phillips DM, Haut RC. The use of a non-ionic surfactant (P188) to save chondrocytes from necrosis following impact loading of chondral explants. J Orthop Res 2004;22(5):1135-42.
33. Rundell SA, Baars DC, Phillips DM, Haut RC. The limitation of acute necrosis in retro-patellar cartilage after a severe blunt impact to the *in vivo* rabbit patello-femoral joint. J Orthop Res 2005;23(6):1363-9.
34. Beecher BR, Martin JA, Pedersen DR, Heiner AD, Buckwalter JA. Antioxidants block cyclic loading induced chondrocyte death. Iowa Orthop J 2007;27:1-8.
35. Martin JA, McCabe D, Walter M, Buckwalter JA, McKinley TO. N-acetylcysteine inhibits post-impact chondrocyte death in osteochondral explants. J Bone Joint Surg Am 2009;91(8):1890-7.
36. Goodwin W, McCabe D, Sauter E, Reese E, Walter M, Buckwalter JA, et al. Rotenone prevents impact-induced chondrocyte death. J Orthop Res 2010;28(8):1057-63.
37. Moussavi-Harami F, Mollano A, Martin JA, Ayoob A, Domann FE, Gitelis S, et al. Intrinsic radiation resistance in human chondrosarcoma cells. Biochem Biophys Res Commun 2006;346(2):379-85.
38. Lee JW, Lim TH, Park JB. Intradiscal drug delivery system for the treatment of low back pain. J Biomed Mater Res A;92(1):378-85.
39. Mollica L, De Marchis F, Spitaleri A, Dallacosta C, Pennacchini D, Zamai M, et al. Glycyrrhizin binds to high-mobility group box 1 protein and inhibits its cytokine activities. Chem Biol 2007;14(4):431-41.
40. Fiedler J, Etzel N, Brenner RE. To go or not to go: Migration of human mesenchymal progenitor cells stimulated by isoforms of PDGF. J Cell Biochem 2004;93(5):990-8.
41. Jiang Y, Jahagirdar BN, Reinhardt RL, Schwartz RE, Keene CD, Ortiz-Gonzalez XR, et al. Pluripotency of mesenchymal stem cells derived from adult marrow. Nature 2002;418(6893):41-9.
42. Seol D, Choe H, Zheng H, Jang K, Ramakrishnan PS, Lim TH, et al. Selection of reference genes for normalization of quantitative real-time PCR in organ culture of the rat and rabbit intervertebral disc. BMC Res Notes 2011;4:162.
43. Kucia M, Reca R, Miekus K, Wanzeck J, Wojakowski W, Janowska-Wieczorek A, et al. Trafficking of normal stem cells and metastasis of cancer stem cells involve similar mechanisms: pivotal role of the SDF-1-CXCR4 axis. Stem Cells 2005;23(7):879-94.

44. Wolff DA, Stevenson S, Goldberg VM. S-100 protein immunostaining identifies cells expressing a chondrocytic phenotype during articular cartilage repair. J Orthop Res 1992;10(1):49-57.
45. Bao JP, Chen WP, Wu LD. Lubricin: a novel potential biotherapeutic approaches for the treatment of osteoarthritis. Mol Biol Rep;38(5):2879-85.
46. Jay GD, Fleming BC, Watkins BA, McHugh KA, Anderson SC, Zhang LX, et al. Prevention of cartilage degeneration and restoration of chondroprotection by lubricin tribosupplementation in the rat following anterior cruciate ligament transection. Arthritis Rheum;62(8):2382-91.
47. Teeple E, Elsaid KA, Jay GD, Zhang L, Badger GJ, Akelman M, et al. Effects of supplemental intra-articular lubricin and hyaluronic acid on the progression of posttraumatic arthritis in the anterior cruciate ligament-deficient rat knee. Am J Sports Med;39(1):164-72.
48. Hunziker EB, Rosenberg LC. Repair of partial-thickness defects in articular cartilage: cell recruitment from the synovial membrane. J Bone Joint Surg Am 1996;78(5):721-33.
49. Wang Q, Breinan HA, Hsu HP, Spector M. Healing of defects in canine articular cartilage: distribution of nonvascular alpha-smooth muscle actin-containing cells. Wound Repair Regen 2000;8(2):145-58.

Table. Relative gene expression. Positive and negative fold change (Δ) for CPC versus NC (left) and CPC versus MSC (right) are shown together with p values (italics). The list includes genes expressed at levels that were at least 2-fold higher (top) or lower (bottom) than in CPC.

Gene Symbol	CPC v NC	
	Δ	p value
IL6	**130**	*3.6E-05*
DOCK10	**62**	*4.4E-07*
CXCL8	**36**	*3.0E-03*
CCNB1	**35**	*5.8E-05*
CXCL12	**28**	*2.4E-05*
CSF1	**21**	*9.3E-06*
MMP1	**18**	*3.9E-03*
CD44	**12**	*6.1E-03*
ADAMTS4	**10**	*2.9E-05*
IL1RN	**9.1**	*1.3E-04*
CCND1	**9.0**	*2.3E-05*
NOTCH1	**7.4**	*9.4E-07*
ADAM9	**6.4**	*1.6E-03*
IGFBP3	**5.6**	*2.7E-02*
MMP13	**4.3**	*1.2E-02*
HMMR	**4.2**	*1.4E-04*
TLR3	**3.7**	*3.7E-02*
ITGB5	**3.6**	*4.0E-02*
COL6A1	**3.1**	*1.1E-02*
ADAM8	**3.0**	*2.0E-02*
COL10A1	**-192**	*7.0E-06*
CHAD	**-136**	*1.5E-08*
COL9A2	**-38**	*4.9E-06*
COL2A1	**-12**	*9.8E-06*
TIMP4	**-8.3**	*9.4E-05*
ACAN	**-8.0**	*5.2E-03*
INSR	**-6.0**	*1.7E-03*
COMP	**-5.4**	*4.9E-04*
TIMP4	**-4.8**	*9.7E-04*
FGF2	**-3.9**	*3.2E-04*
ACAN	**-3.7**	*3.2E-02*
PTH1R	**-3.1**	*1.8E-02*
DNMT3A	**-2.9**	*2.3E-02*

Gene Symbol	CPC v MSC	
	Δ	p value
PRG4	**78**	*7.6E-05*
MMP3	**23**	*1.0E-03*
ACAN	**17**	*5.4E-04*
S100A1	**16**	*2.7E-04*
MMP1	**15**	*5.2E-03*
HAPLN1	**13**	*1.0E-05*
S100A1	**13**	*1.7E-04*
CXCL2	**12**	*2.0E-02*
IL8	**10**	*2.5E-02*
COL2A1	**6.9**	*8.0E-05*
SOD3	**6.7**	*1.3E-04*
COL5A3	**6.2**	*1.5E-03*
FGF2	**5.1**	*8.6E-05*
IL16	**3.3**	*8.5E-03*
CD83	**3.2**	*1.5E-02*
PLAT	**3.0**	*4.2E-02*
SOCS1	**2.7**	*2.2E-02*
IL1A	**2.7**	*2.2E-02*
S100B	**2.6**	*1.6E-03*
PDGFRA	**2.5**	*8.4E-03*
SOD2	**2.3**	*3.4E-02*
NID1	**-11**	*4.4E-02*
IGFBP7	**-10**	*6.7E-03*
PPARG	**-9.8**	*5.3E-03*
THBS1	**-6.5**	*4.2E-02*
GPC4	**-6.2**	*1.8E-02*
IGFBP3	**-5.4**	*4.6E-02*
IGFBP2	**-3.6**	*1.0E-02*
IL1RN	**-3.6**	*4.3E-03*
PLAU	**-3.0**	*2.0E-03*
DNMT3A	**-2.7**	*1.1E-02*
IGFBP4	**-2.6**	*2.6E-02*
NOTCH1	**-2.3**	*6.2E-04*

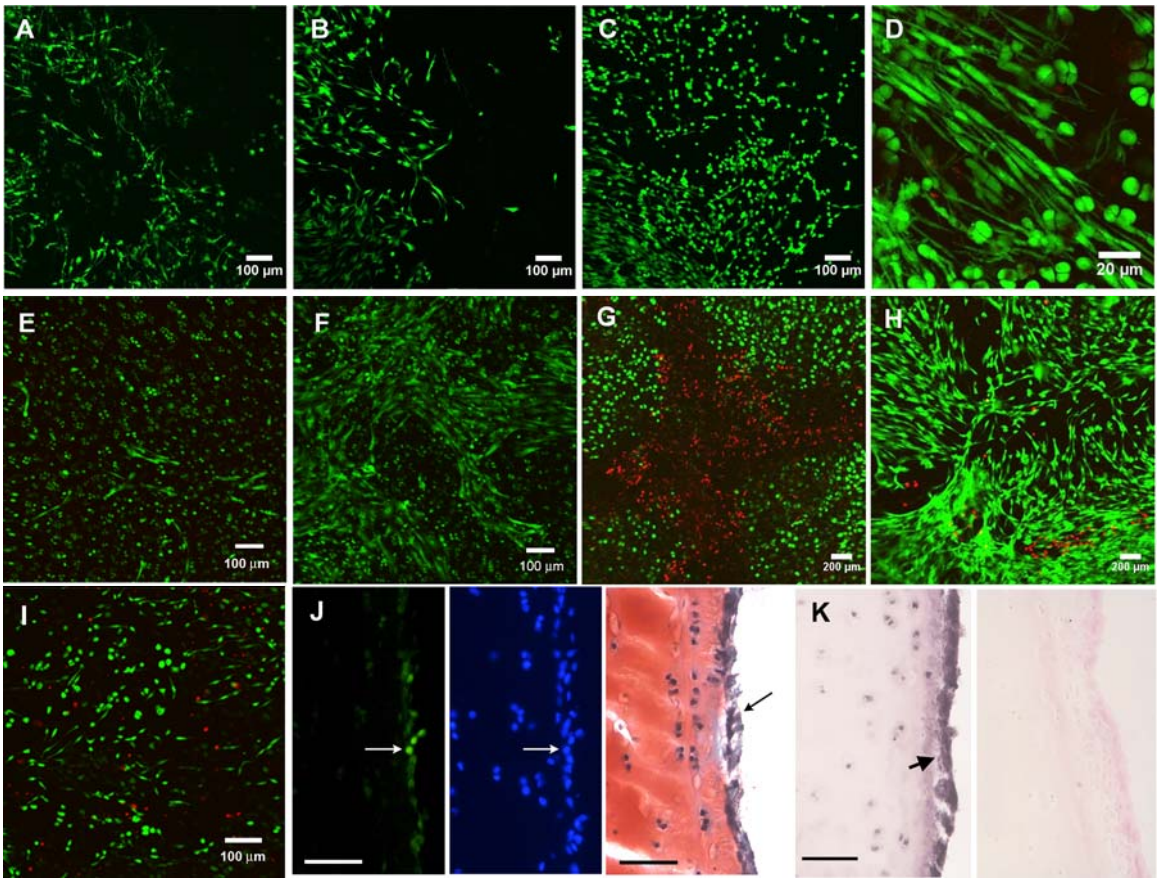

Figure 1. Migrating cells on injured cartilage. (A-C) Confocal images show live cells (green) in the same area within an impact site on the surface of a explant at day 7 (A), 11 (B), and 15 (C) post-impact. The elongated morphology and dendritic appearance of the cells are shown in a high magnification view (D). Live cells were found on a human talus from a 36 year old male at day 6 (E) and 10 (F) post-impact. Dead cells (red) and live cells in a bovine explant with a cross-shaped needle scratch imaged immediately after the injury (G) and 14 days later (H). Migrating cells were observed on the surfaces of cartilage dissected free from subchondral bone immediately after impact (I). (J) Green immunofluorescence staining for PCNA reveals positive cells (arrow) on the surface of a cartilage explant (left panel). The blue staining (middle panel) shows all nuclei in the same section. Surface-migrating pCPCs (arrow) can be seen in a consecutive section stained with safranin-O/fast green (right panel). (K) Immunohistochemical staining for lubricin. The arrow on the left points to strongly positive migrating cells in an impact site. The right panel shows a negative control. Bars (J and K)=100 microns.

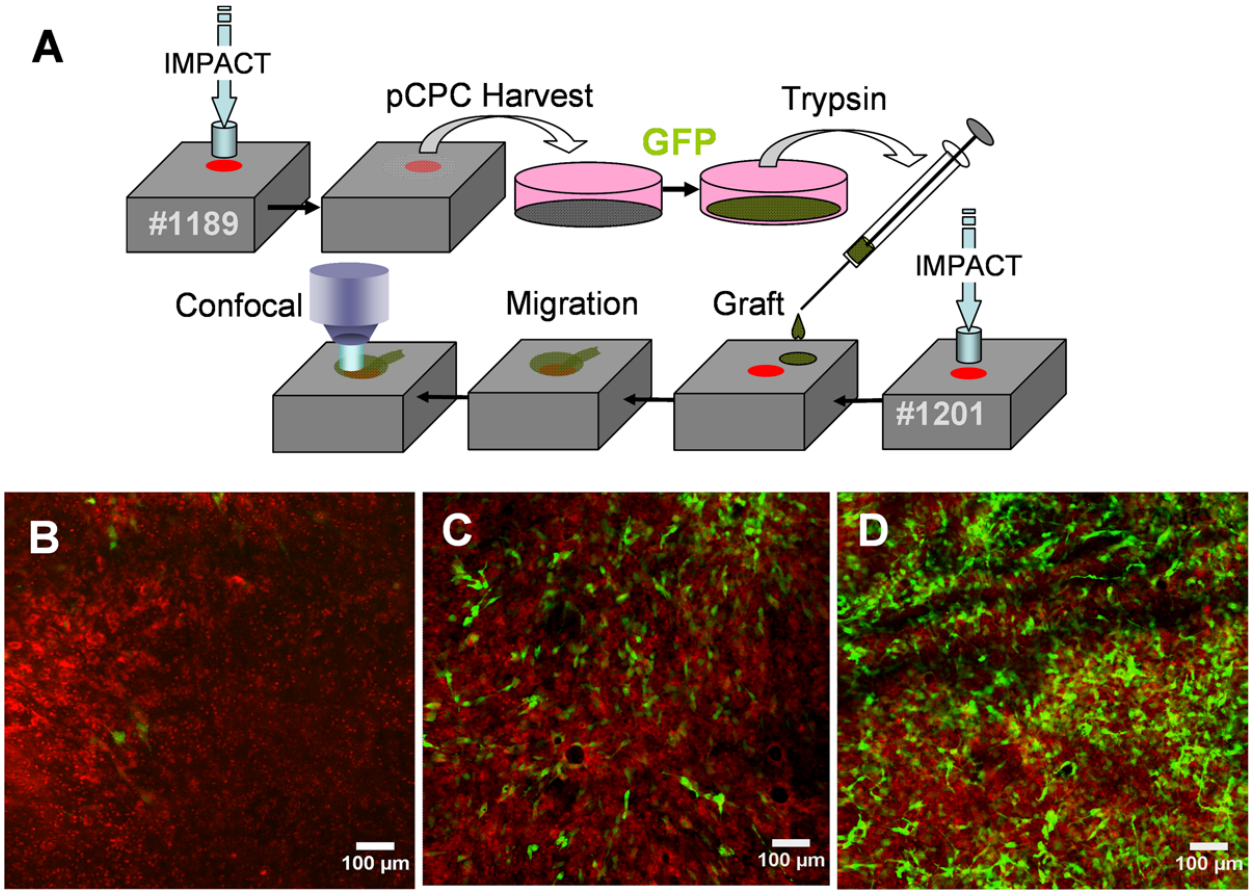

Figure 2. Migration of grafted pCPCs. (A) Procedure for harvesting and grafting pCPCs. The boxes represent two different explants (specimen #1189 and specimen #1201). Explant 1189 was impacted and incubated for 5 days to allow pCPCs to emerge. These cells were harvested and placed in monolayer culture for GFP transduction. Labeled cells were trypsinized, suspended in a temperature-sensitive hydrogel, and grafted onto explant 1201, which had been impacted a few hours earlier. The impact site was imaged by confocal microscopy at various times after grafting. Grafted GFP-labeled cells (green) can be seen against the background of host cells labeled with a red tracking stain. Exactly the same field within the impact site was imaged at 2 days (B), 5 days (C), and 12 days (D) post-grafting.

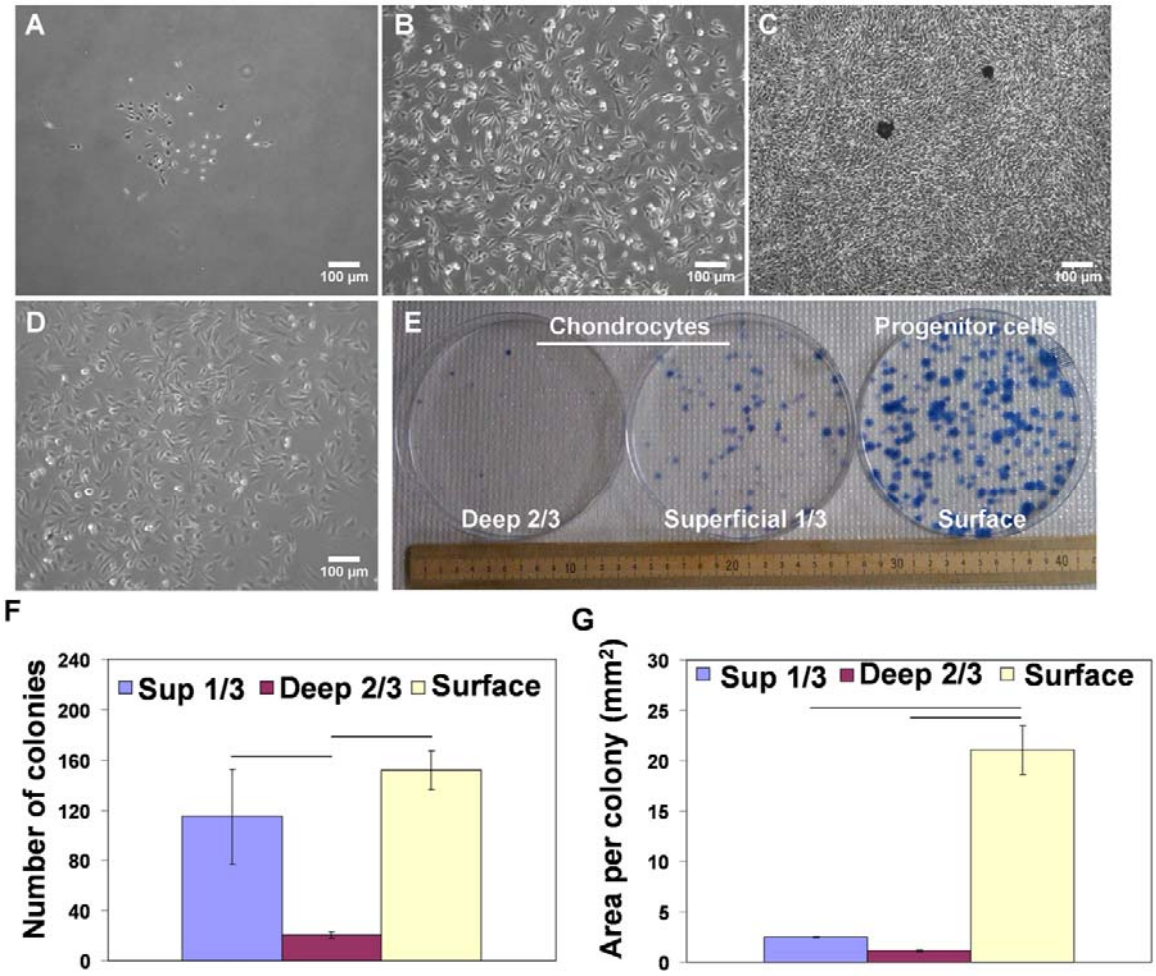

Figure 3. Colony formation by migrating progenitor cells and chondrocytes. (A-D) Light microscope image of single colony of progenitor cells at 2 days (A), 3 days (B), and 6 days (C) after seeding. Image of a chondrocyte colony cultured for 13 days (D). (E) Macroscopic image of cloning plates seeded with chondrocytes from the deep and superficial zones or progenitor cells after 10 days of growth. The total number of colonies (F) and average colony area (G) were measured using ImageJ. Progenitor cells and superficial chondrocytes showed higher numbers of colonies than deep chondrocytes. However, colony area was much larger for progenitor than chondrocytes from either zone. p values are shown. Columns and error bars are means and standard deviations based on n=4-5 different batches of cells.

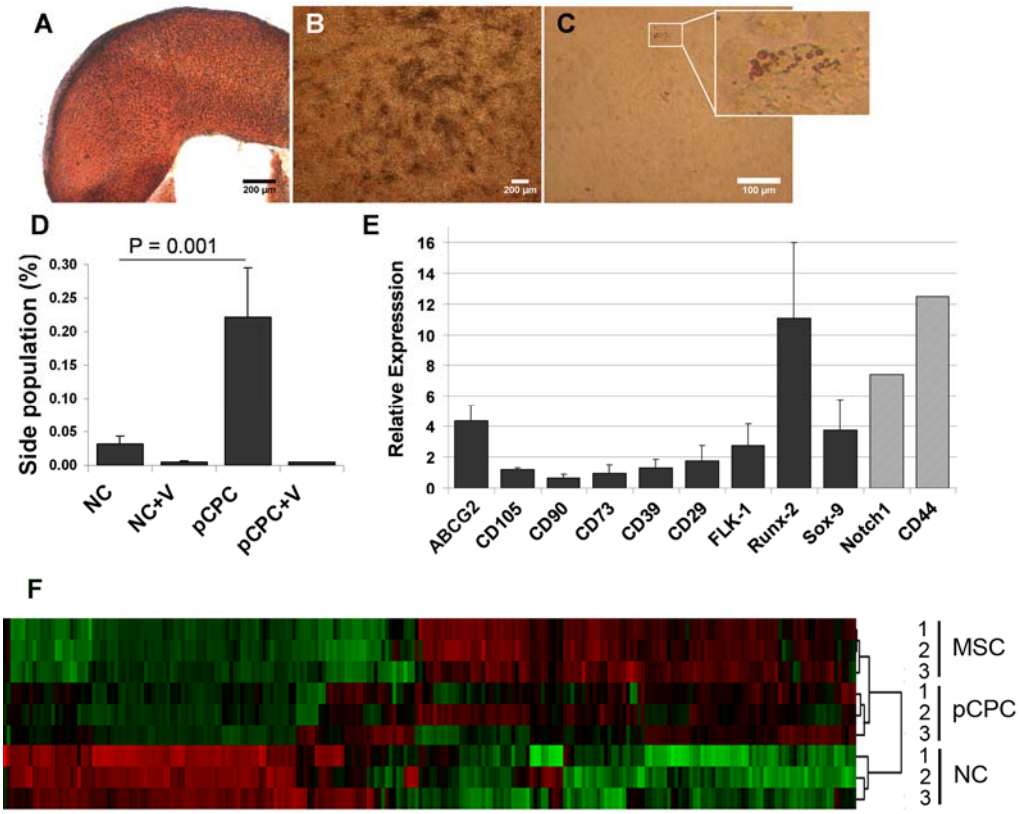

Figure 4. pCPCs show stem cell characteristics (A-C) pCPCs were cultured under chondrogenic (A), osteogenic (B), and adipogenic (C) conditions. The pellet culture showed intense red Safranin-O/fast green staining indicating the presence of cartilage proteoglycans. (B) Deposition of calcium phosphate was detected by staining with Alizarin Red (dark red spots). (C) Only a few cells produced positive fat vacuoles in Oil Red O staining. (D) FACS analysis showed that the proportion of side population was significantly higher in progenitor cells than in chondrocytes (p=0.001). As expected Verapamil (V), an ABCG transport inhibitor, ablated the side population. (E) The graph shows real-time PCR analysis (dark columns) and microarray analysis (light columns) of marker gene expression in pCPCs relative to NCs (fold change). (F) A heatmap and dendrogram summarize microarray data for the indicated cell populations (triplicate analyses). Colored bars show genes that were expressed at higher or lower levels than the median value (green and red respectively). The dendrogram on the right indicates that CPCs and MSCs were more closely related to each other than to NCs.

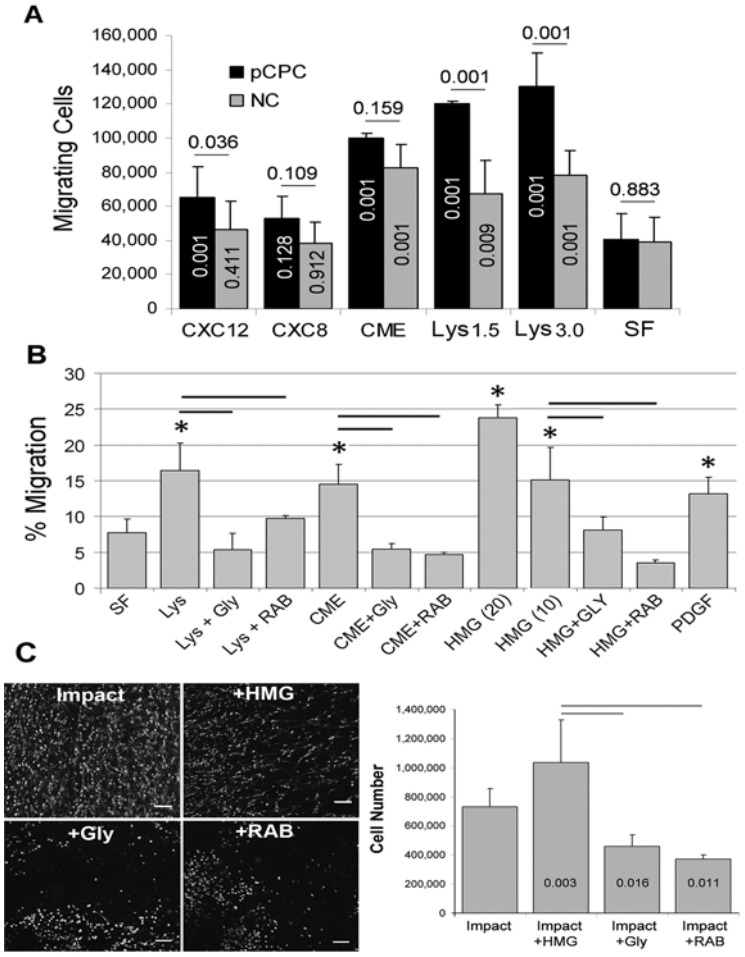

Figure 5. Chemotactic activity. (A) The columns show numbers of cells that responded to CXCL12, CXCL8, conditioned medium (CME), cell lysates (Lys) made from 1.5 x 10^6 cells (1.5) and 3.0 x 10^6 cells (3.0), or serum-free medium (SF). The numbers above the bars indicate p values for differences between pCPC and NC. Numbers within columns are p values for differences between treatments and SF. (B) Effects of glycyrrhizin (Gly) and anti-RAGE antibody (RAB) on responses to CME, Lys (3.0 x 10^6 cells), and HMGB1 [HMG (10)= 10 nM, HMG (20) =20 nM] on pCPC chemotaxis (% Migration). Columns and error bars are means and standard deviations (n = 3-9). Asterisks indicate p values of less than 0.005 for treated versus SF (one-way ANOVA). (C) Confocal images show results for an untreated impacted control (Impact) and for impacted explants treated with HMGB1 (+HMG), glycyrrhizin (+Gly), and anti-RAGE antibody (RAB). Bars = 100 μm. The histogram on the right shows means and standard deviations for yields of migrating cells (n=4/group). p values (versus Impact-only) are indicated in the columns. Horizontal bars show significant differences between the HMG-treated and Gly-treated groups and between the HMG-treated and RAB-treated groups (p = 0.001).